

A High-Resolution Electron Micrograph of the Twin Boundary in Pyrite

BY G. DONNAY AND J. D. H. DONNAY

Department of Geological Sciences, McGill University, 3450 University Street, Montreal, Quebec, Canada H3A 2A7

AND SUMIO IJIMA

Department of Physics, Arizona State University, Tempe, Arizona 85281, USA

(Received 8 November 1976; accepted 2 February 1977)

Minute fragments of an iron-cross twin of pyrite containing the twin boundary were studied by high-resolution electron microscopy with electron-diffraction control. Bright-field images show, looking down \mathbf{c} , two mutually perpendicular sets of dark equidistant fringes (one set for each crystal in the twin) arising from interference of the 000 beam with the dynamically scattered 100 reflexions. The fringes of each set are 5.4 Å (one cell edge) apart. In each crystal the fringes are perpendicular to the [010] direction and hence to the macroscopic striations on (001), which are parallel to the edge (102):(102). Where the two crystals overlap and the fringes intersect to give a square net, the boundary surface can be seen. It is three-dimensional, irregular, consisting of planar rectangular regions parallel to the cube faces, $ma \times na \text{ Å}^2$ in area, where integers m and n range from 1 to ~ 25 . No evidence was found for defects or impurity atoms at the twin boundary. On the atomic scale the twin operation is a glide reflexion, with glide component equal to $(\mathbf{a}_1 + \mathbf{a}_2)/2$, in a (110) plane passing through point $0, \frac{1}{2}, 0$; but the arrangement of the S_2 doublets along the twin glide plane remains indeterminate. The iron lattice complex F is coherent throughout the twin.

Introduction

The morphology of penetration twins raises the question of how two or more crystals, readily told apart where they emerge from their 'common volume', are distributed and separated inside this volume. What is the nature of the twin-boundary surface? Is it two or three-dimensional? Is it composed of planar regions on an atomic scale? Is it a locus of high defect density, and are these defects two or three-dimensional? Are impurity atoms concentrated near the contact, as have been observed at grain boundaries? Another question concerns the twin law: what direct evidence can be obtained on the twin operation on the atomic scale?

X-ray and electron diffraction give no answer to any of these questions. According to classical theory (Friedel, 1904, 1926), a penetration twin is to be expected when the *twin lattice* is the crystal lattice (as it is in pyrite) or one of its superlattices. It follows that the diffraction pattern of such a twin simulates only one reciprocal lattice, and it is well known (see, for instance, Cowley, 1976) that the Bragg intensities are not measurably affected by the twin boundary. High-resolution electron microscopy (Pierce & Buseck, 1976) may well provide answers to such questions.

Experimental

An iron-cross twin of pyrite composed of two interpenetrating {210} dihexahedra [crystal symmetry $2/m\bar{3}$ and twin symmetry $4'/m\bar{3}2'/m'$, Curien & LeCorre (1958), Curien & Donnay (1959)], was chosen as a promising sample to be investigated. The high stability

of pyrite in the electron beam makes this sulphide preferable to quartz, which also shows penetration twinning. From a thin section cut parallel to (001), pieces including twin boundaries were selected and ground in a mortar to fragments of μm size. The fragments were searched for traces of twin boundaries at low magnification. On a bright-field image (taken with only the 000 beam), the contour lines due to variation of the thickness (Fig. 1) show some discontinuities across the twin boundary running vertically near the centre of the fragment. An electron-diffraction pattern of a region covering the boundary comes from both crystals of the twin (Fig. 2a). Weak reflexions $hk0$ with both h and k odd, such as 110, which are among those forbidden by the space group $P2_1/a\bar{3}$ and are forbidden by the twin, are due to the phenomenon of multiple reflexion, common for the short-wavelength electrons. They arise when the electron waves pass through regions near the twin boundary where the crystals I and II are superimposed. This has been confirmed by examining a dark-field image taken with one of the 110 reflexions.

In the bright-field images the forward scattered 000 beam and 100 reflexions pass through the objective aperture which is placed symmetrically on the optical axis of the objective lens. Fringes arise from interference of the kinematically forbidden 100 reflexions with the 000 beam and so are visible only in the thicker part of the specimen (more than $\sim 50 \text{ Å}$ thick) where the 100 reflexions acquire appreciable amplitude as a result of dynamical scattering.

Because the complicated dynamical scattering leaves unknown the phase relations of the 100 reflexions and

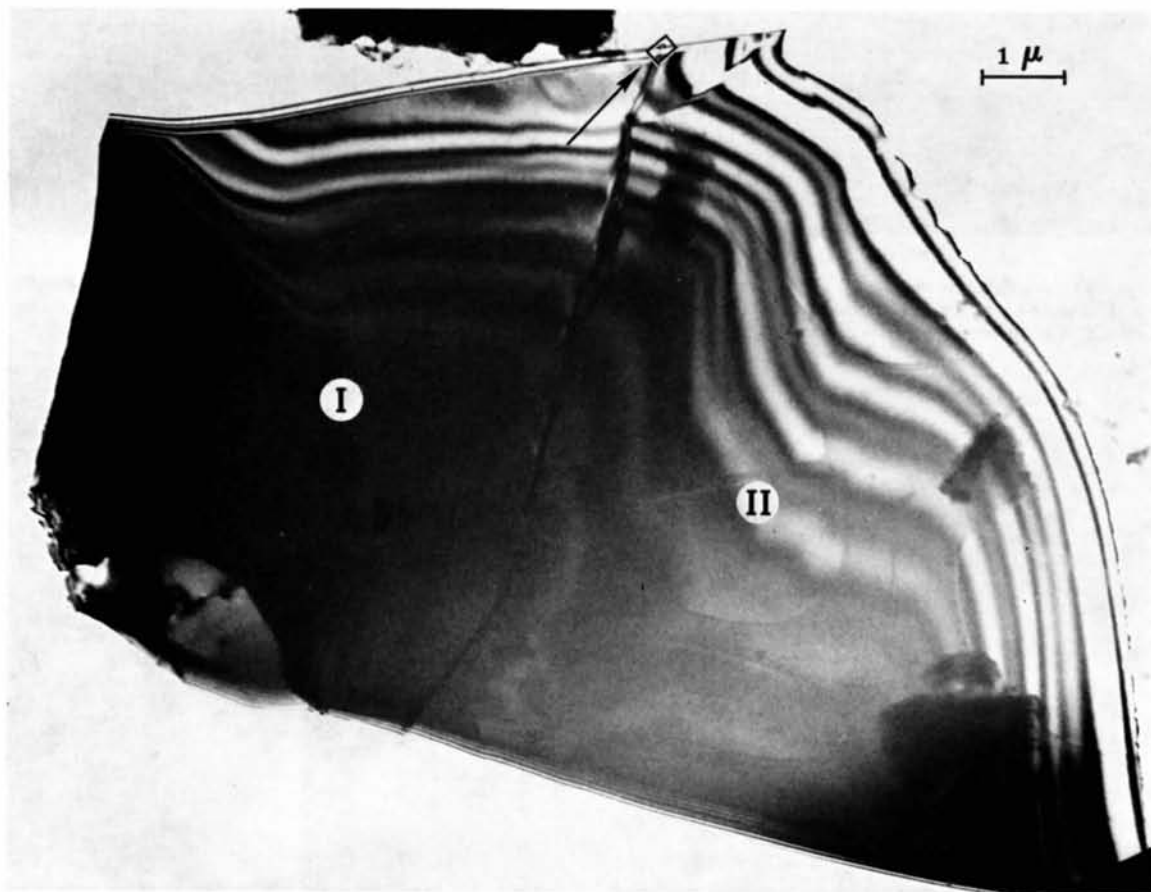


Fig. 1. Low-magnification electron micrograph of a pyrite-twin fragment showing twin boundary, which appears as a dark band running N-S.

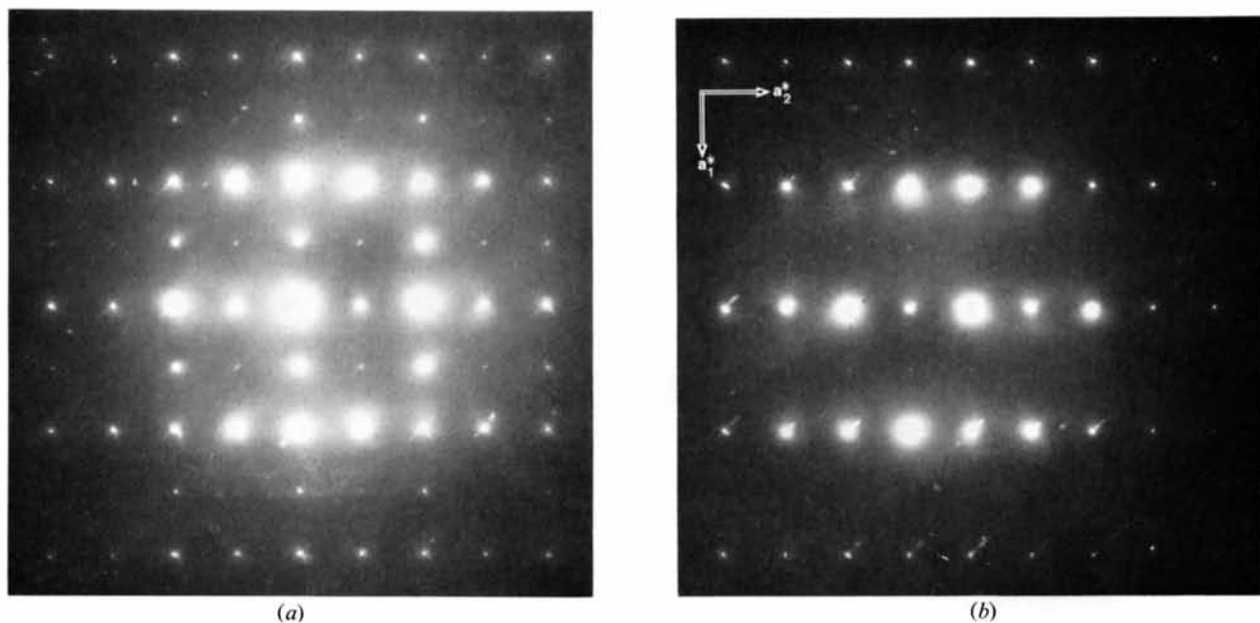


Fig. 2. (a) Electron-diffraction pattern $(001)_0^*$ showing $hk0$ reflexions from a region of the twin boundary in the fragment shown in Fig. 1. Two sets of $hk0$ reflexions, one from each crystal, are superimposed. Note forbidden reflexions $hk0$ with both h and k odd, due to multiple reflexion. (b) Electron-diffraction pattern from a region of crystal I in Fig. 1.

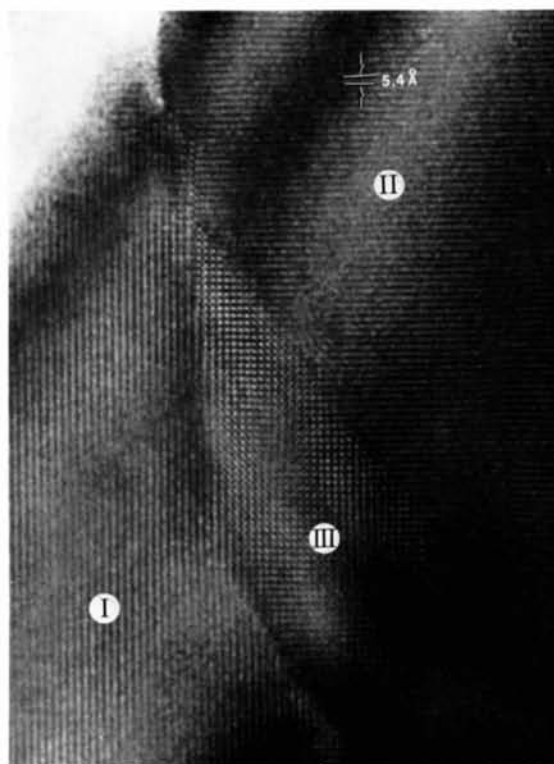


Fig. 3. High-resolution electron micrograph from twin-boundary region enclosed by rectangle in Fig. 1. Lattice fringes are N-S in crystal I, E-W in crystal II. The spacing of the fringes, 5.4 \AA , corresponds to the interplanar distance obtained from the 100 dynamical reflexions. In region III, where the two crystals overlap, the fringes cross, showing that the twin boundary is not a plane parallel to (010) , but an irregular surface.

the incident beam, the position of the dark fringes with respect to the positions of atoms in the unit cell is not uniquely determined. However, since the orientation of the incident beam relative to the lattice is very nearly the same for both crystals in the twin, it may safely be assumed that the position of the dark fringes in the unit cell is the same in the two cases. Hence an arbitrary correlation of the dark fringe with any particular plane of the structure will be permissible.

The high-resolution electron micrograph (Fig. 3) taken of the twin boundary near the edge of the crystal (enclosed in Fig. 1) shows fringes one cell edge (5.4 Å) apart, lying north-south (N-S) in crystal I (lower left) and east-west (E-W) in crystal II (upper right). The contact surface is irregular, but it is made up of *mutually perpendicular steps equal to 5.4 Å or multiples thereof*. Where the two crystals overlap in projection (region marked III), the fringes intersect to give a square net in the [001] projection (Fig. 3). The E-W fringes meet the N-S fringes in such a way that they always terminate exactly on a N-S fringe, never halfway between two adjacent N-S fringes. The same is true of the N-S fringes that end on an E-W fringe. It follows that the two lattices I and II are coherent (or 'in phase') with each other. These observations thus yield the first *direct* experimental evidence of the twin lattice, predicted long ago by twinning theory (Friedel, 1904, 1926), but heretofore confirmed only in its consequences.

Comparison of the fringe pattern from crystal I with the corresponding (001)₀ electron-diffraction pattern, which contains the *hk0* reflexions (Fig. 2*b*), shows that the fringes are perpendicular to the \mathbf{a}_2^* direction and thus parallel with the [100] rows. We know from the pyrite structure that these rows are those on which the S₂ groups project in the same orientation, either NW-SE or NE-SW. It will be recalled that the macroscopic striations on the cube faces have been correlated with the crystal structure (Bragg & Claringbull, 1965): on (001) they are parallel to the \mathbf{a}_2 direction, that is, the edge (102):(102). *The fringes on the electron micrograph are therefore perpendicular to the macroscopic striations.*

The many micrographs that we have examined all show only one twin boundary in a field several thousand Å across; repeated twinning was not observed on the micrographs.

The twin operation on the atomic scale

As long as only the point-group symmetry of a macroscopic crystal is considered, the operation that describes the pyrite iron-cross twin is any one of the 24 symmetry operations that belong to the cubic holohedral group $4/m\bar{3}2/m$ (lattice symmetry), but not to its hemihedral subgroup† $2/m\bar{3}$ (crystal symmetry). Indeed

all 24 operations, applied simultaneously, bring crystal I to coincidence with crystal II. Note that all symmetry elements and twin elements are made to pass through the origin, which is the fixed point in the point group.

On the atomic scale, however, the twin operation is not necessarily a reflexion (or a rotation): it can entail a glide of one half (or some other fraction) of a lattice translation, in combination with the reflexion (or the rotation). Moreover, the position of the twin element (twin mirror, twin glide plane, twin rotation axis, twin screw axis or twin centre) in the crystal structure must be specified.

Some atoms form a lattice complex‡ that extends throughout the twin and remains invariant under the operations of its own symmetry, which may be higher than that of the space group of the structure. The twin operations are among those symmetry operations of the said lattice complex that do not belong to the space-group symmetry. The lattice complex thus plays the role of the 'twin lattice' of the classical theory. In pyrite there are two such lattice complexes: (1) all the iron atoms form the *F* lattice complex, with symmetry *Fm3m*, in standard representation, one point at 0, 0, 0; (2) all the sulphur doublets are centred on the points of the *F* lattice complex, shifted by vector $\frac{1}{2}, \frac{1}{2}, \frac{1}{2}$ to representation $\frac{1}{2}, \frac{1}{2}, \frac{1}{2}F$; the sulphur atoms themselves, however, are displaced from these points in the direction of a body diagonal of the cube (one for each doublet), and they obey symmetry *Pa3*. One of the four doublets, centred at 0, 0, $\frac{1}{2}$ for instance, can be taken invariant under the twin operation; only the remaining three will change orientation in twinning.

Consider (Fig. 4) a schematic representation of the pyrite crystal structure [$a=5.40$ Å, $P2_1/a\bar{3}$, $Z=4$ (Bragg, 1913)] projected along *c*. The origin is placed at an iron atom (under the S₂ doublet in the upper left corner). Every sulphur doublet is figured by an arrow that points toward the upper sulphur atom. An arrow with a black head has its midpoint at $z=0$; one with a white head, at $z=\frac{1}{2}$. The arrows are parallel to the body diagonals of the cubic cell. On the drawing, the twin boundary appears as a broken line consisting of steps that have been taken equal for convenience. The N-S lines in crystal I (lower left) are parallel to the observed fringes on Fig. 3; corresponding lines in crystal II (upper right) must accordingly lie E-W.

Noting that the 'flight of stairs' follows the (110) net plane, we draw two straight lines, *AA* and *BB*, that enclose the steps. The slab thus defined is occupied partly by crystal I and partly by crystal II. The sulphur doublets whose centres project on *AA* and *BB* belong, respectively, to crystal I and crystal II. (Note, however, that half of these doublets have the same orientation in I and II.) A third line, *CC*, halfway between the first two, is the trace of the *twin glide plane* (110) through point $0, \frac{1}{2}, 0$, with glide component $(\mathbf{a}_1 + \mathbf{a}_2)/2$, which

† The old mineralogical concept of *hemihedry* in this case coincides with that of *subgroup of index 2* in modern parlance.

‡ Readers unfamiliar with this concept are referred to Fischer, Burzlaff, Hellner & Donnay (1973).

was first proposed for pyrite by Strunz & Tennyson (1965) and which, we see, can indeed be used to describe the twin. All the S_2 doublets whose centres project on AA or to the left of it are related to the doublets whose centres project on BB or to the right of it by the *twin glide reflexion*, which, for the complex of iron atoms considered by itself, is a reflexion in (110) followed by an F -lattice translation $[\frac{1}{2}\frac{1}{2}0]$, two operations that leave it invariant. Finally consider the S_2 doublets whose centres project on the trace CC of the twin glide plane, at midpoints of mesh edges, alternately on the tread and on the riser of the steps. These doublets cannot satisfy both crystals, since this constraint would require *two* doublets to be centred at each such midpoint – a sterically impossible configuration.

One plausible hypothesis consists in choosing those arrows that project along the CC line, so that the S_2 doublets lie in the twin glide plane, belong alternately to crystals I and II, and are all in one and the same orientation, which is compatible with crystal II on the tread of the step and with crystal I on its riser (Fig. 4). [This hypothesis is the only one that was considered by Strunz & Tennyson (1965), who regard the atomic lamella along CC as a 'marcasite lamella'.]

A second hypothesis selects the arrows that project perpendicularly to the CC line; the S_2 doublets lie in vertical planes at rightangles to the twin glide plane. Successive doublets could be in alternate orientations, one obeying crystal I on the tread, the other obeying

crystal II on the riser, or *vice versa*; instead of being ordered, the doublets could be disordered, the two possible orientations being equally represented.

A third hypothesis can be entertained: every S_2 doublet along CC is solicited to adopt two different orientations, that of crystal I and that of crystal II; it could settle in the intermediate orientation, which projects on a N–S arrow on the riser and on a W–E arrow on the tread. Such a phenomenon was postulated once before (Donnay, Kullerud & Donnay, 1971) to provide a mechanism for the marcasite-to-pyrite transformation.

Whereas in the first hypothesis the S_2 doublets have their long axes contained in the twin glide plane, in the second and third hypotheses only their centres lie on CC in $(1\bar{1}0)$. Of the three hypotheses, none can be proved experimentally at this time. Even the imaging technique would be powerless: on previous electron-microscope images of sulphides (Pierce & Buseck, 1976), cations show up well, but sulphur atoms are not visible. Whichever hypothesis is correct, however, the *shared slab* of the twin, parallel to the twin glide plane ($1\bar{1}0$), consists of only one *shared structural plane*, the trace of which is the line CC (Fig. 4). This shared plane is 'shared' in a quite literal sense, since each of the two crystals contributes half the sulphur doublets whose centres lie in the plane.

The antiphases

In the generalization of the point-group theory of twinning proposed by Donnay & Curien (1960), in which pyrite is used as an example, it is recognized that some of the additional symmetry operations of $Fm\bar{3}m$ (symmetry of the iron lattice complex) over $Pa\bar{3}$ (symmetry of the pyrite space group) lead to the twinned orientation and its antiphases, while some produce the antiphases of the original structure. It is also pointed out, in the same paper, that, in a *twin* (meaning the complex edifice), two *macroscopic crystals* intervene, I and II, each of which is made up of antiphase domains.

The overall coherence of the iron lattice complex, in standard representation F , symmetry $Fm\bar{3}m$, with concomitant coherence of the lattice complex of the *midpoints* of the S_2 doublets, in shifted representation $\frac{1}{2}, \frac{1}{2}, \frac{1}{2}F$, can exist with eight distinct configurations of the *sulphur* doublets. These are (Fig. 5): (1) the configuration chosen to describe the known crystal structure of pyrite in space group $Pa\bar{3}$; (2), (3), (4) the three antiphases thereof; (5) the configuration of crystal II in its twin relation to crystal I; (6), (7), (8) the three antiphases thereof. The antiphase vectors are $0, \frac{1}{2}, \frac{1}{2}, \frac{1}{2}, 0, \frac{1}{2}, \frac{1}{2}, 0$ for cases (2) and (6), (3) and (7), (4) and (8), respectively.

It is clear from the projection that the N–S rows of sulphur doublets are shifted, by one half of the cell edge, from (1) to (2) and from (1) to (4), whereas in (3) they remain in their original positions. It follows that, in crystal I, the lattice fringes will likewise be shifted by $a/2$, in cases (2) and (4), whereas case (3) will be in-

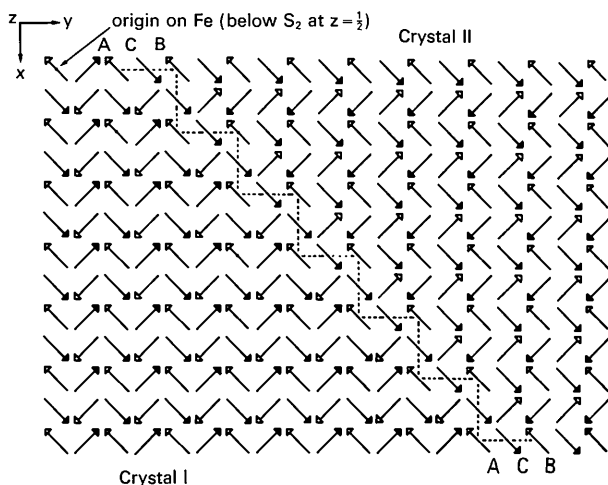


Fig. 4. Projection (001) of the structure of a pyrite twin. The origin is chosen on an iron atom (at $z=0$). Only the sulphur doublets are shown; they are represented by arrows pointing up along body diagonals; the doublet midpoint is at $z=0$ or $z=\frac{1}{2}$ accordingly as the arrowhead is black or white. An idealized twin boundary is shown as a flight of stairs (*dotted*). The contact slab between crystals I and II projects between lines AA and BB ; the shared structural plane, along CC . In reality the steps of the stairs are random multiples of 5.4 \AA on risers and treads, so that the line CC splits into irregularly displaced parallel segments, all of which remain coherent (or 'in phase'). The riser and the tread of the steps shown here are in zone [001]; similar steps, in zones [100] and [010], also form part of the irregular three-dimensional surface.

distinguishable from (1). In crystal II the system of coordinates, being obtained from that of I by a reflexion, is left handed. The situation in projection is the same as for crystal I, except that the rows of sulphur doublets, and the corresponding lattice fringes, are oriented E-W: cases (6) and (8) show the shift; case (7) cannot be distinguished from (5).

The phenomenon was actually observed in the (001) projection, both in crystal I and in crystal II. The antiphase vector, in each crystal, can be either $0, \frac{1}{2}, \frac{1}{2}$ or $\frac{1}{2}, \frac{1}{2}, 0$; this indeterminacy cannot be resolved from the data of a single projection. All that can be said is that crystal I shows the following configurations: (1), with or without (3), producing the main set of diffraction fringes, and (2) or (4) or both, accounting for the set of 'halfway' fringes. Likewise, in crystal II the main fringes and the offset fringes are accounted for by (5) with or without (7), in the former case, and by (6) or (8) or both, in the latter.

To produce a shift of the lattice fringes in crystal I in such a way that it can be observed in the (001) projection, the antiphase vector must contain a component $a_2/2$, a condition that is satisfied by vectors $0, \frac{1}{2}, \frac{1}{2}$ and $\frac{1}{2}, \frac{1}{2}, 0$. The question arises, can $0, \frac{1}{2}, 0$ be an antiphase

vector? If it were, in either crystal of the twin, its effect would be the same as that of $0, \frac{1}{2}, \frac{1}{2}$ or $\frac{1}{2}, \frac{1}{2}, 0$ (Fig. 5) and would be observable in the shift of the lattice fringes. Vector $0, \frac{1}{2}, 0$, however, would also bring about an interchange of the iron ions and the sulphur doublets, thus yielding crystallochemically awkward contacts and destroying the coherence of the iron lattice complex, which extends through each crystal (and even across the twin boundary between them).

One last remark: combining translation $0, \frac{1}{2}, 0$ with a reflexion, in the hope of finding a possible twin operation, results in a crystal-symmetry operation, *viz* a glide reflexion in glide plane *a* of the *Pa3* space group.

Conclusions

In pyrite penetration twinning, the twin operation is a glide reflexion in a plane (110) passing through a point $(p, q + \frac{1}{2}, 0)$, *p* and *q* integers, with glide component $(a_1 + a_2)/2$, as was proposed by Strunz & Tennyson (1965). The twin-boundary surface is irregular, distinctly three-dimensional; it consists of mutually perpendicular planar regions, $ma \times na \text{ \AA}^2$ in area, that contain $m \times n$ square cell faces, where integers *m* and *n* range from 1 to ~ 25 . The lattice fringes show no evidence of any high density of defects or impurity atoms near the twin boundary, so that the contact surface should not represent a local region of high energy, and repeated twinning might be expected. Although, as mentioned above, we did not observe it on a microscopic scale, repeated twinning is known on macroscopic twins. The two opposite terminations of one of the two macroscopic crystals in the penetration twin of pyrite need not be connected through the central region to scatter coherently; this conclusion follows from the coherence of the iron lattice complex across the twin boundary (observed in the *x* and *y* directions, hence inferred for the *z* direction). There is thus no reason to refrain from describing such a twin as being composed of two single crystals, where a 'single crystal' comprises two or more distinct regions in parallel orientations. Each such region comprises at least two antiphases (observed) and possibly two more.

For a direct determination of the twin operation, the fringe method used here in the case of pyrite bids fair to be serviceable for other penetration twins, when the imaging method fails to bring out some critical atomic groups.

We are deeply indebted to Professor J. M. Cowley, Arizona State University, for many discussions and much help in the interpretation of the micrographs and in the presentation of the manuscript, especially in the experimental section. Our thanks are also due to Mrs Louise Stephenson, Redpath Museum of McGill University, for providing the pyrite twin (specimen No. F615), to Mr R. Wise for preparing the thin sections that were later ground to slivers for electron microscopy, and to our McGill colleague Dr Yvon Le Page

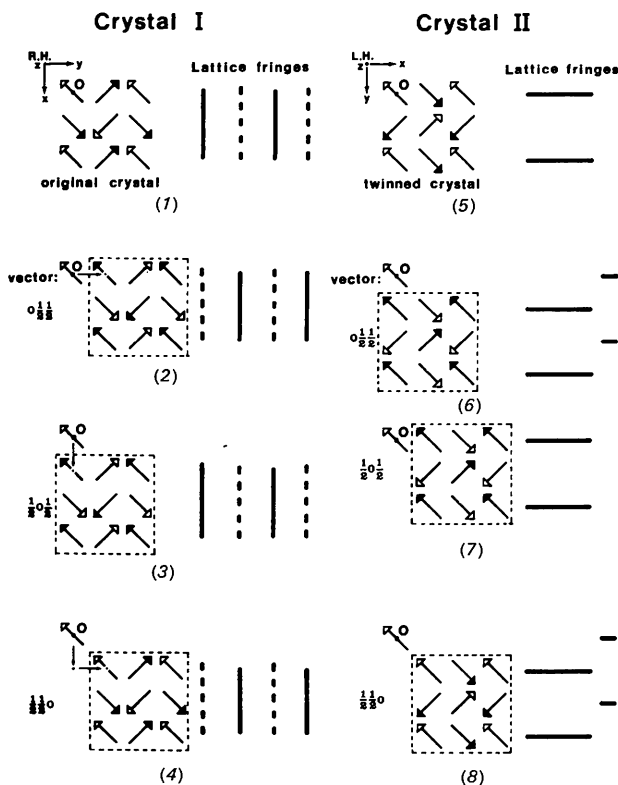


Fig. 5. Projection on (001) of the four antiphases of crystal I [(1) to (4)] and of crystal II [(5) to (8)]. The origin of (1) is shown on projections (2), (3), (4); that of (5), on drawings (6), (7), (8). The positions of the lattice fringes are indicated by heavy lines. Antiphases (5) to (8) of crystal II are obtained by twinning of antiphases (1) to (4) of crystal I.

for a critical reading of the manuscript. GD received financial support from the National Research Council (Canada) and the Ministère de l'Éducation (Quebec); SI, from the National Science Foundation (USA) through Grant DMR 76-06108.

We tender very special thanks to a referee for his remark that an antiphase vector $\frac{1}{2}, \frac{1}{2}, 0$ should result in a discontinuity of the fringes: on reexamining our photographs we actually observed the phenomenon in both crystals of the twin.

References

- BRAGG, W. L. (1913). *Proc. Roy. Soc. A* **89**, 468–489.
 BRAGG, W. L. & CLARINGBULL, G. F. (1965). *Crystal Structures of Minerals*, p. 67. Ithaca: Cornell Univ. Press.
 COWLEY, J. M. (1976). *Acta Cryst.* **A32**, 83–87, 88–91.
 CURIEN, H. & DONNAY, J. D. H. (1959). *Amer. Min.* **44**, 1067–1070.
 CURIEN, H. & LECORRE, Y. (1958). *Bull. Soc. Fr. Minér. Crist.* **81**, 126–132.
 DONNAY, J. D. H. & CURIEN, H. (1960). *Inst. Lucas Malladas, Cursillos Conf.* **7**, 13–14.
 DONNAY, J. D. H., KULLERUD, G. & DONNAY, G. (1971). *Trans. Amer. Cryst. Assoc.* **7**, 69–76.
 FISCHER, W., BURZLAFF, H., HELLMER, E. & DONNAY, J. D. H. (1973). *Space Groups and Lattice Complexes*. Monograph 134, US National Bureau of Standards, Washington, D.C.
 FRIEDEL, G. (1904). *Etude sur les groupements cristallins*. *Bull. Soc. Ind. Minér. St-Etienne*, (4) **3** and **4**. Reprinted in book form.
 FRIEDEL, G. (1926). *Leçons de Cristallographie*. Paris: Berger-Levrault. Reprint (1964); Paris: Blancard.
 PIERCE, L. S. & BUSECK, P. R. (1976). *Applications of Electron Microscopy in Mineralogy*, edited by H. R. WENK, p. 137. New York: Springer.
 STRUNZ, H. & TENNYSON, CH. (1965). *Neues Jb. Miner. Mh.* pp. 247–248.

Acta Cryst. (1977). **B33**, 626–628

On the Refinement of Atom–Atom Potential Parameters in Molecular Crystals

BY G. TADDEI, R. RIGHINI AND P. MANZELLI

Istituto di Chimica-Fisica, Università di Firenze, via G. Capponi, 50121 Firenze, Italy

(Received 7 February 1977; accepted 22 February 1977)

The refinement of atom–atom parameters for molecular crystals has been considered. A simple formalism is developed for reducing the time taken for numerical computations and ensures reliable results. This formalism consists in defining independent potential parameters and deriving physically meaningful relations between the parameters which refer to the 'mixed' atom–atom interactions and other parameters. This procedure was applied to four aromatic hydrocarbon crystals; however it can be generalized to any molecular crystal with any molecule with any number of heteroatoms.

In recent years the atom–atom model was certainly the leading model for the intermolecular interactions in molecular crystals. This model was extensively applied to the calculation of several crystal properties (Schnepp & Jacobi, 1972). Among the atom–atom potentials, the Buckingham functions have been used the most successfully. A typical Buckingham potential function is the following

$$V(r) = A \exp(-Br) - Cr^{-6} \quad (1)$$

where A , B and C are variable parameters and r is the distance between two atoms belonging to different molecules ('non-bonded atoms'). Nine different parameters are to be defined for the hydrogen–hydrogen ($H \cdots H$), carbon–hydrogen ($C \cdots H$) and carbon–carbon ($C \cdots C$) interactions of a hydrocarbon crystal. Very reliable sets of these parameters were obtained by Williams (1966) on the basis of a refinement procedure which was performed considering the crystal sublimation energy and the lattice equilibrium conditions with respect to the unit-cell parameters, the molecular orientations

and displacements of the molecule's centre of mass.

Williams (1966) refined independently five out of the nine necessary parameters, *i.e.* A_{HH} , A_{CH} , A_{CC} , C_{HH} and C_{CC} , whereas B_{HH} , C_{CH} , B_{CC} are fixed *a priori* and C_{CH} is assumed to equal the geometric mean of C_{HH} and C_{CC} . The validity of this procedure is debatable for two reasons: (i) A , B and C are not actually independent of each other, (ii) A , B and C of the 'mixed' $C \cdots H$ interactions can be connected with the parameters of the interactions $H \cdots H$ and $C \cdots C$ by more suitable relations.

Point (i) is clarified by writing (1) in the form:

$$V(r) = \frac{\varepsilon}{\mu - 1} \left\{ \exp \left[-6\mu \left(\frac{r}{\varrho} - 1 \right) \right] - \mu \left(\frac{\varrho}{r} \right)^6 \right\} \quad \text{with } \mu > \frac{7}{6} \quad (2)$$

where ϱ and ε are respectively the equilibrium distance and the equilibrium potential depth of the function and μ is its 'steepness' (Hirschfelder, Curtiss & Bird, 1954). The condition $\mu > \frac{7}{6}$ arises because the function $V(r)$